Available online at www.sciencedirect.com
SCIENCE DIRECT
Polymer 46 (2005) 11396–11406
polymer
www.elsevier.com/locate/polymer

Morphology of PEO/PDMS blends during shear: Coexistence of two droplet/matrix structures and additive effects

Verena E. Ziegler, Bernhard A. Wolf *

Institut für Physikalische Chemie der Johannes Gutenberg-Universität, Jakob-Welder-Weg 13, D-55099 Mainz, Germany

Received 13 September 2005; accepted 4 October 2005
Available online 27 October 2005

Abstract

The morphologies of blends of polyethyleneoxide (PEO 37) and poly(dimethylsiloxane)s (PDSM), with viscosity ratios, λ, of approximately one (PDMS 230) or 2.8 (PDMS 314, being the component of higher viscosity) and interfacial tensions on the order of 10 mN/m, were investigated at 70 °C as a function of shear rate (up to 10 s^{-1}) and of time. For the system PEO 37/PDMS 230 we have also studied the influence of the compatibilizer dimethyl–ethyleneoxide–copolymer (PDMS-*co*-PEO), which is only reasonably soluble in PEO. To investigate the morphologies we have used an optical shear cell in combination with a light microscope. The most important observation consists in the formation of two coexisting droplet/matrix structures for volume fractions of PDMS ranging from 0.4 to 0.6 for both λ values; the presence of the copolymer extends this region to 0.7. In the case of $\lambda \approx 1$ the average droplet radii are within experimental error independent of composition and morphology; for $\lambda = 2.8$ they depend on the matrix phase in which they are contained and do again not vary with composition. The reduction in drop size caused by the copolymer is markedly larger if PEO forms the matrix. The present morphological observations suggest that the two coexisting droplet/matrix phases develop out of a single droplet/matrix structure via coalescence processes.

Keywords: Polymer blends; Morphology under shear; Phase inversion

1. Introduction

The morphology of blends between incompatible polymers depends on numerous variables: composition, viscosities η of the phases, the viscosity ratio λ, the interfacial tension σ, the elasticity and the flow field. At the borders of the concentration axis normally a dispersed droplet/matrix structure is found. The morphology determining processes are breakup and coalescence of drops. Breakup of a single drop has been studied in detail [1–4]. The same holds true for the coalescence of droplets [5–13].

As one adds more of the minor component to a dispersed droplet/matrix structure this material is usually forming continuous structures (and becomes extractable by selective solvents) in addition to the existing droplet/matrix structure [14–16]. The corresponding characteristic composition, where this process sets in is called percolation threshold φ_c. As one increases the amount of the minor component still further, matrix and dispersed phase change their role at the volume fraction of phase inversion φ_I. At this point it is impossible to decide, which phase constitutes the matrix and which one the dispersed phase. For such co-continuous structures it is possible to reach each part of a given phase without leaving this phase. With polymer blends one usually finds a region of co-continuity instead of one characteristic composition of phase inversion [14–19].

Two possible mechanisms are discussed in literature for the building of co-continuous structures [20]: coalescence of (more or less elongated) drops [19,21,22] or via formation of sheets [23–26]. This study was undertaken to investigate the stationary state morphologies of a model blend consisting of polyethyleneoxide and poly(dimethylsiloxane). In the course of these experiments we also obtained some information on the time development of these morphologies.

2. Experimental

Polyethyleneoxide PEO 37 was purchased from Roth, Germany; the two poly(dimethylsiloxane)s (PDMS 230 and PDMS 314) were donated by Wacker, Germany and a dimethyl–ethyleneoxide–copolymer (PDMS-*co*-PEO) by Goldschmidt, Germany. The numbers after the abbreviations

* Corresponding author. Tel.: +49 6131 3922491.
E-mail address: bernhard.wolf@uni-mainz.de (B.A. Wolf).

0032-3861/$ - see front matter © 2005 Elsevier Ltd. All rights reserved.
doi:10.1016/j.polymer.2005.10.017

Table 1
Molar masses (as obtained from GPC measurements), viscosities and densities of the polymers

	PDMS 230	PDMS 314	PEO 37
M_n/kg mol^{-1}	67	126	34
M_w/kg mol^{-1}	234	314	459
$\eta^{70\,°C}$/Pa s	142	459	161.5
ρ/g cm^{-3}	0.9921–8.54× $10^{-4}t$/°C		1.1479–8.52× $10^{-4}t$/°C

are the weight average molar mass of the polymers in kg/mol. The molar masses were determined by means of the GPC in dimethylformamide using PEO standards for PEO and in toluene with PDMS-standards for PDMS. The results are shown in Table 1. The structure of the copolymer was clarified by ^{1}H NMR-measurements, together with information supplied by the manufacturer. The formula is shown in Fig. 1.

The polyethyleneoxide sample melts at 65 °C, therefore, the temperature for the measurements was chosen to be 70 °C. The viscosities at this temperature were measured with the rotational rheometer AR 1000 from Thermal Analysis, US. PDMS 230 behaves Newtonian up to shear rates $\dot{\gamma} = 5\ s^{-1}$, PDMS 314 up to 3 s^{-1} and PEO 37 at least up to 20 s^{-1}. The zero shear viscosities are listed in Table 1.

The interfacial tension of PEO 37/PDMS 230 with and without copolymer was determined by means of the pendant drop method [27,28]. Apparatus and procedures are described elsewhere [29]. The experiments were carried out at different temperatures as a function of time until a constant value for the interfacial tension was reached. This could last from several minutes up to three days depending on temperature and additive concentration. The density of PEO 37 was measured in 5 °C steps between 70 and 100 °C with a pycnometer, the density of PDMS 230 was obtained by means of a commercialized apparatus (DMA 48, Paar Physica, Austria) between 20 and 70 °C in steps of 10 °C. The results are displayed in Table 1. The interfacial tension of the pure system depends on temperature in the following manner: σ/mN m^{-1} = 10.62–1.1×10^{-2}t/°C.

The copolymer is only in small amounts soluble in PEO and practically immiscible with PDMS. The change of the density of the PEO-phase due to the copolymer added is negligible. For the calculation of the interfacial tension the density of the pure PEO was used aside from the measurement with the pure copolymer.

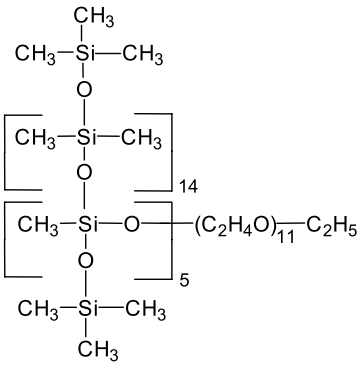

Fig. 1. Chemical structure of PDMS-*co*-PEO.

The morphology was investigated by means of the optical shear cell CSS 450 from Linkam Scientific, GB. It consists of a plate/plate geometry made by glass. The cell is inserted into an optical microscope BX50, Olympus, Japan. The microscope is equipped with a B/W CCD-camera M10 from JAI, Denmark. The direction of observation is perpendicular to the plane of shear. The images were digitized and analyzed with the software Optimas 6.1 from Media Cybernetics, USA.

The samples were prepared in the following manner: the crude mixture of the components was put into an oven at 90 °C to melt the PEO. Then it was stirred with a spatula by hand for 2 min, placed back into the oven and vacuum was applied to remove air bubbles. This lasts about 10 to 20 min. After that the sample was filled into the shear cell and pre-sheared for 5 min at 15 s^{-1} to annihilate the prehistory. A step down of the shear rate to the requested shear rates followed. This step down defines the start of the time axis. At 5 s^{-1} the gap was set 100 μm, at 2 s^{-1} 250 μm and at 1 s^{-1} 400 μm, to ensure that wall effects are absent.

To determine the drop size in the quiescent state, the shear was stopped several times for about 20–30 s, to allow the relaxation of the drops and to take images at different locations in the gap. During this period of observing the stagnant mixtures one can see both, coalescence of drops and break up of highly elongated drops/threads within the region of medium concentrations. To obtain the average drop size we have normally at least evaluated 200 drops except for those cases, where the images did not show enough drops; in this case the smallest number was about 60 drops. The number average drop radius R_N and the volume average radius R_V were calculated according to Eqs. (1) and (2). The drop size distributions were fitted according to Gauss (Eq. (3)), giving R_G.

$$R_N = \frac{\sum_{i=1}^{\infty} n_i R_i}{\sum_{i=1}^{\infty} n_i} \tag{1}$$

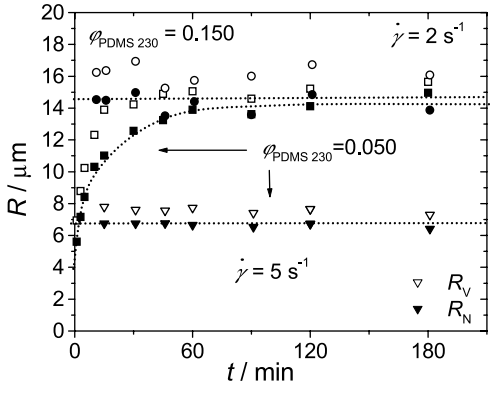

Fig. 2. R_N (solid symbols) and R_V (open symbols) for $\varphi_{PDMS230}$=0.05 (5 s^{-1}: triangle, 2 s^{-1}: square) and for $\varphi_{PDMS230}$=0.15 (2 s^{-1}: circle) as a function of time. The lines for R_N are drawn as guide for the eye.

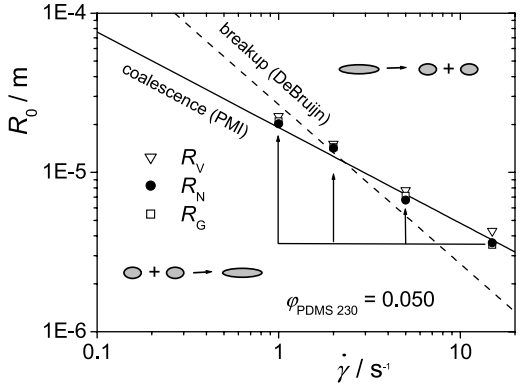

Fig. 3. Elmendorp diagram for $\varphi_{PDMS230}=0.050$.

$$R_V = \frac{\sum_{i=1}^{\infty} n_i R_i^4}{\sum_{i=1}^{\infty} n_i R_i^3} \tag{2}$$

$$y = y_0 + \frac{A}{SD\sqrt{2\pi}} e^{(R-R_G)^2/2SD^2} \quad SD: \text{standard deviation} \tag{3}$$

In some cases it was not clear at the temperature of observation which polymer should be assigned to which part of the morphology. Therefore, the samples were cooled to room temperature at the end of the coalescence experiments and polarized light was used to distinguish between the crystalline PEO and the PDMS melt. In order to avoid possible changes in the morphology that could take place during the cooling of the systems at rest, the mixtures were sheared down to 60 °C, i.e. close to the onset of the crystallization of the PEO, which starts at about 58–55 °C.

3. Results and discussion

3.1. PEO 37/PDMS 230 ($\lambda \approx 1$)

Three examples of the development of drop size with time are shown in Fig. 2 for $\varphi_{PDMS230}=0.050$ at 2 and 5 s^{-1}, respectively, and for $\varphi_{PDMS230}=0.150$ at 2 s^{-1}. Only for the first example and the lower shear rate the radii change with time. The reason for this lies in the coalescence probability. For low concentrations and low shear rates this quantity is small, which means that it takes more time to reach the steady state value. An increase in concentration results in an augmentation of the number of drops and so does, therefore, the collision probability. Increasing the shear rate acts in the same direction because more collisions take place per time unit. For $\varphi_{PDMS230}=0.050$ an influence of time on drop size was observed at $\dot{\gamma}=2$ and 1 s^{-1}. For 5 s^{-1} time dependence was absent for all compositions studied, as well as for 2 s^{-1} except for $\varphi_{PDMS230}=0.050$.

From the time independent drop radii at different $\dot{\gamma}$ it is possible to determine the coalescence curve according to the model of partially mobile interface [30,31] (Eq. (4)), which had turned out to be appropriate for most polymer blends [8,32–34]

$$R = \left(\frac{16}{3}\right)^{1/5} \left(\frac{h_{crit}}{\lambda}\right)^{2/5} \left(\frac{\eta_m \dot{\gamma}}{\sigma}\right)^{-3/5} \tag{4}$$

with η_m being the matrix viscosity, $\lambda=\eta_d/\eta_m$ and h_{crit} the critical film thickness for the rupture of the matrix film between to colliding drops. h_{crit} is treated as an adjustable parameter.

The breakup process can be modeled by the equation given by DeBruijn [4], which yields the critical capillary Ca number of breakup for a given λ

$$\log Ca_{crit} = -0.506 - 0.0994 \log \lambda + 0.124(\log \lambda)^2 - \frac{0.115}{\log \lambda - \log 40.8} \tag{5}$$

with the definition of Ca

$$Ca = \frac{\dot{\gamma}\eta_m R}{\sigma} \tag{6}$$

it is possible to calculate the maximum stable drop size as a function of shear rate for a given system, if the matrix viscosity and the interfacial tension are known.

These two curves are displayed conjointly according to Elmendorp [6] as shown in Fig. 3 for $\varphi_{PDMS230}=0.050$. Except

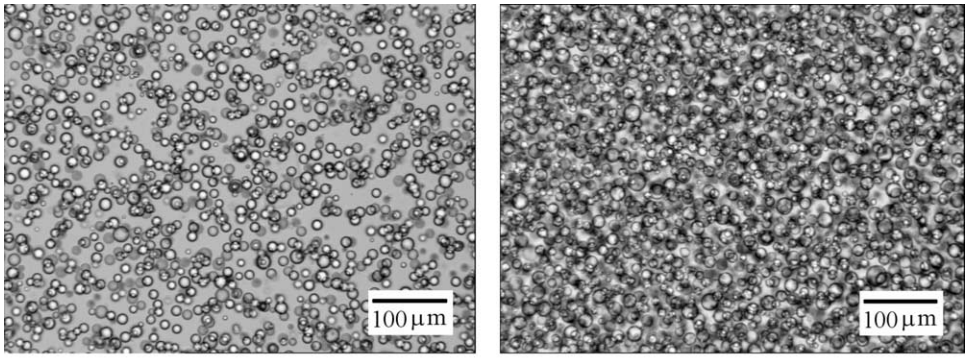

$\varphi_{PDMS\ 230}$ = 0.05 $\varphi_{PDMS\ 230}$ = 0.15

Fig. 4. Light microscopic images of PEO 37/PDMS 230 taken after 1 h shearing at $\dot{\gamma}=5$ s^{-1} for different blend compositions. The shear was stopped immediately before taking the pictures.

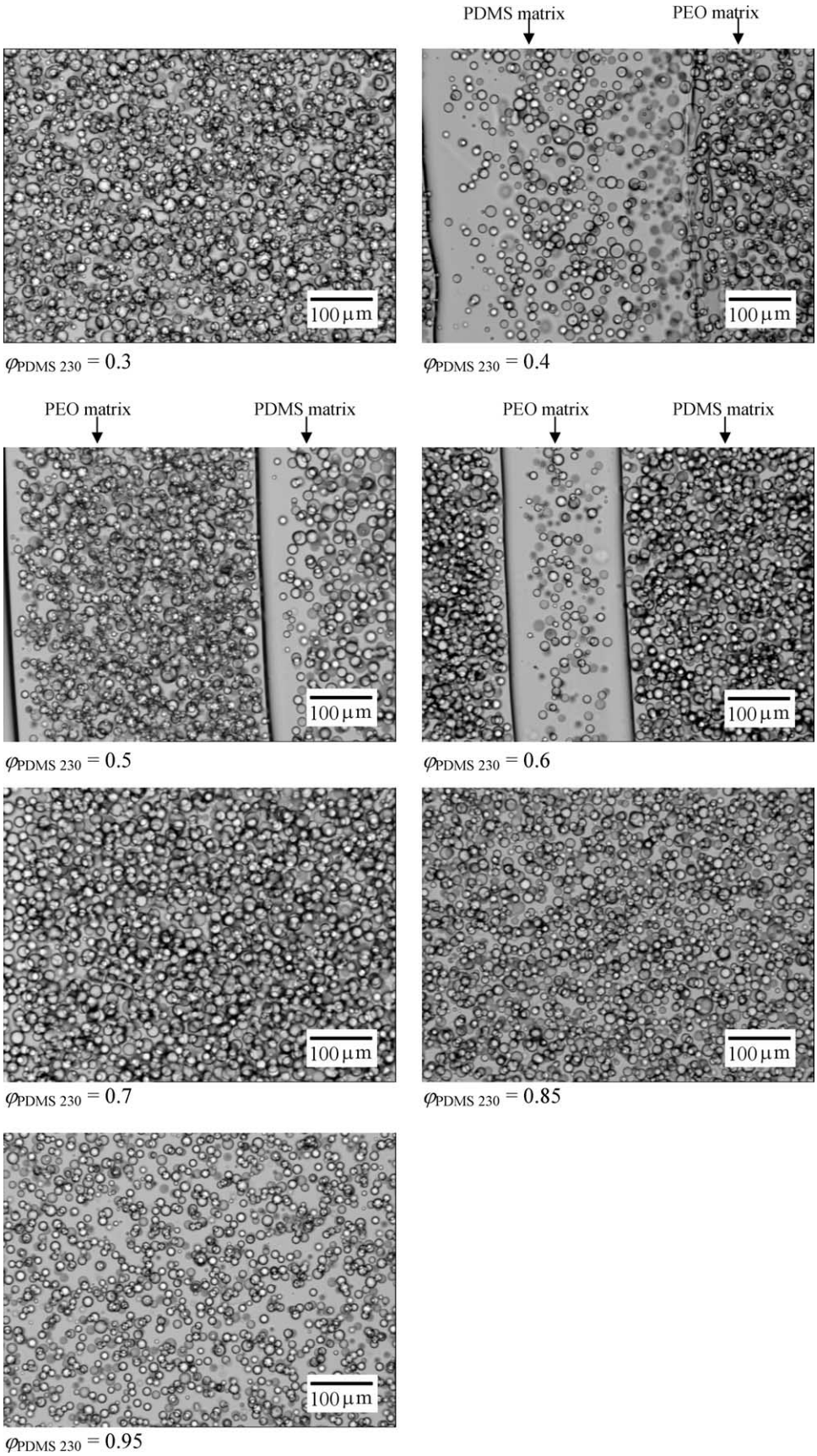

Fig. 4 (*continued*)

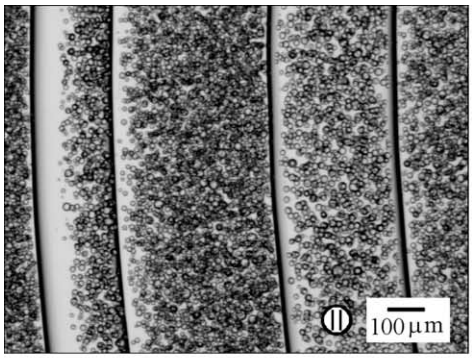

$\dot{\gamma} = 0\ s^{-1}$ after shearing at $5\ s^{-1}$; 70°C

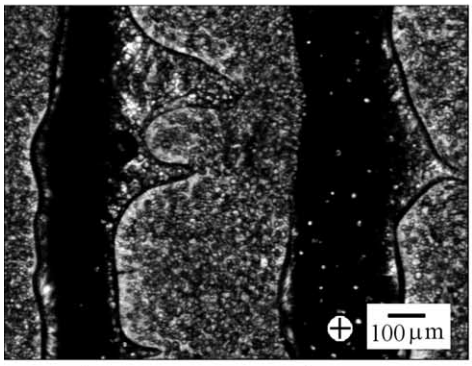

$\dot{\gamma} = 0\ s^{-1}$ after shearing at $5\ s^{-1}$; 30°C

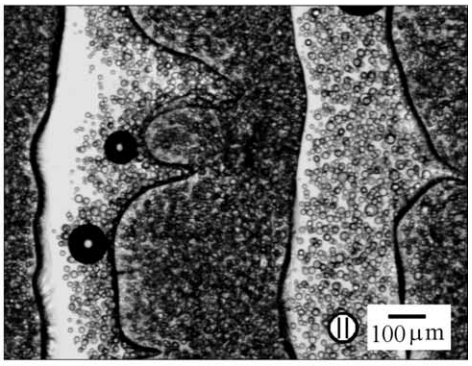

$\dot{\gamma} = 0\ s^{-1}$ after shearing at $5\ s^{-1}$; 30°C

(a)

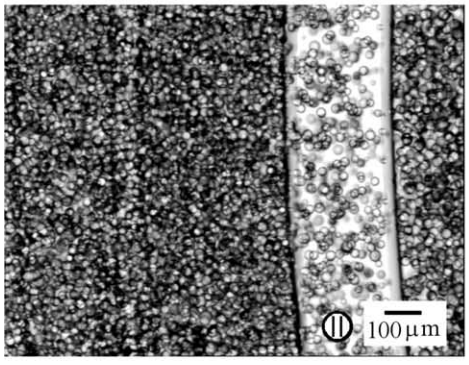

$\dot{\gamma} = 0\ s^{-1}$ after shearing at $2\ s^{-1}$; 70°C

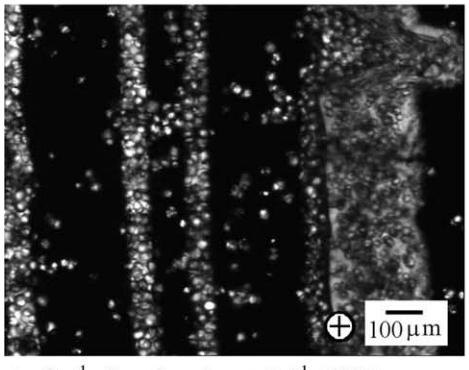

$\dot{\gamma} = 0\ s^{-1}$ after shearing at $2\ s^{-1}$; 30°C

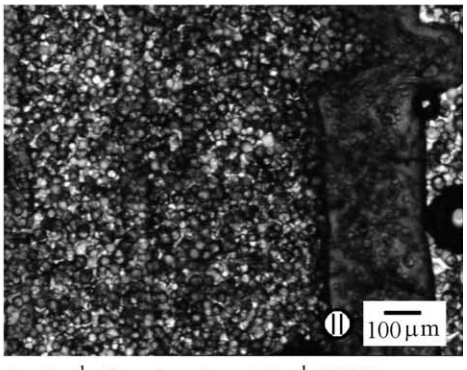

$\dot{\gamma} = 0\ s^{-1}$ after shearing at $2\ s^{-1}$; 30°C

(b)

Fig. 5. Microscopic images of PEO 37/PDMS 230 taken with polarized light after shearing for 2 h. Part a: $\varphi_{PDMS230} = 0.5$; $\dot{\gamma} = 5\ s^{-1}$; part b: $\varphi_{PDMS230} = 0.6$; $\dot{\gamma} = 2\ s^{-1}$. The image in the top left is taken at 70 °C, the lower ones after quenching to room temperature. The signs left of the scales indicate the position of the polarizers.

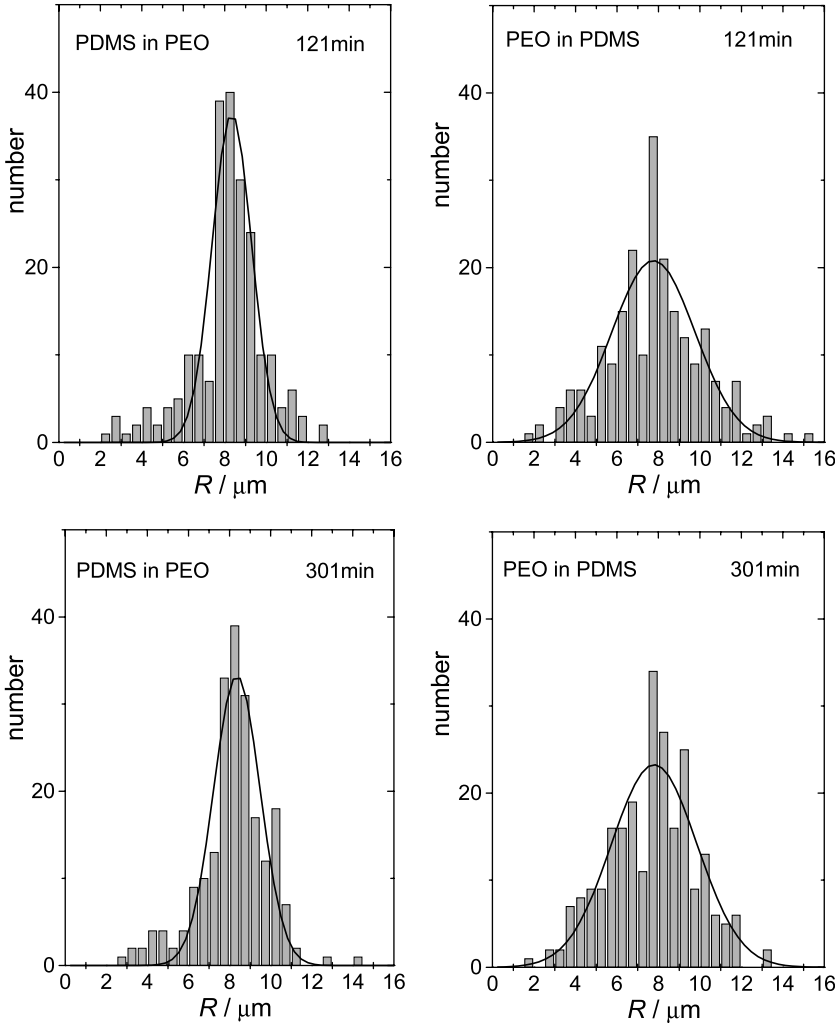

Fig. 6. Drop size distribution of the two droplet/matrix phases for $\varphi_{\mathrm{PDMS\ 230}} = 0.5$ and $\dot{\gamma} = 5\ \mathrm{s}^{-1}$ at the indicated times. The lines are fits according to Gauss (Eq. (3)).

for 1 s^{-1} all average radii lie on or above the breakup line. This means that the drop size for $\dot{\gamma} > 1\ \mathrm{s}^{-1}$ is determined by the establishment of truly stationary states between breakup and coalescence processes.

Fig. 4 displays images of PEO 37/PDMS 230 blends over the whole range of composition; they were obtained as described in the experimental section. The pictures were taken after shearing the blend for one hour at 5 s^{-1}. For $\varphi_{\mathrm{PDMS230}}$ below 0.4 and above 0.6 one droplet/matrix phase is observed, for $0.4 \leq \varphi_{\mathrm{PDMS230}} \leq 0.6$ two inverse droplet/matrix structures appear. The same holds true for $\dot{\gamma} = 2\ \mathrm{s}^{-1}$. From these images it is impossible to decide which phase forms the matrix and which the drops. Cooling the samples to room temperature after the experiments enables such an assignment because PEO crystallizes and can be seen in the polarized light. Two examples are given in Fig. 5(a) and (b). In order to avoid misinterpretations concerning the fraction of PEO the mixtures contain, one should keep in mind that the crystallization is impeded if this polymer constitutes the drops; even

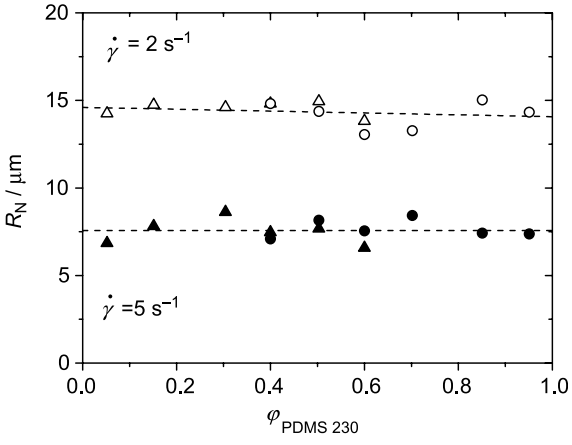

Fig. 7. Stationary drop sizes as a function of composition for PEO 37/PDMS 230 at $\dot{\gamma} = 5$ (solid) and at 2 s^{-1} (open); triangles: PDMS drops in PEO, circles: PEO in PDMS. The lines are drawn as guide for the eye.

after two hours most of the drops may still consists of amorphous PEO.

It is interesting to note that the drop size does practically not vary with composition in the example shown in Fig. 4. Furthermore, as it looks there exists a correlation between the fraction of the total volume a certain structure (PEO drops in PDMS or vice versa) occupies and the drop density in this droplet/matrix morphology.

Fig. 6 shows the drop size distributions for both droplet/matrix phases in case of $\varphi_{\mathrm{PDMS\ 230}} = 0.5$ and $\dot{\gamma} = 5\ \mathrm{s}^{-1}$ after 121 and 301 min. It is possible to fit all data according to Gauss (Eq. (3)). The size distribution of PEO-drops in PDMS is slightly broader than that of PDMS drops in PEO.

The results of the image analysis of the micrographs shown in Fig. 4 are displayed in Fig. 7. The drop sizes are within experimental error the same for all compositions.

3.2. PEO 37/PDMS 314 ($\eta_{PEO}/\eta_{PDMS} = 0.35$)

The influence of the viscosity ratio of the two blend components is studied by changing the viscosity of the PDMS sample. The drop sizes in dependence on composition are depicted in Fig. 8. For PDMS 314-drops in PEO, the mean drop size is the same as for PDMS 230. The explanation lies in the occurrence of two opposing effects: the coalescence radius decreases because λ increases (the matrix viscosity being the same) and the breakup radius rises due to the increasing drop viscosity. In the case of PEO-drops in the PDMS-matrix both effects operate in the same direction: the breakup radius decreases because of the increasing matrix viscosity and so does the coalescence radius (cf. Eq. (4)). This means that the measured drop size for PEO 37-drops in PDMS 314 is smaller than for PDMS 230 as the matrix. Extension and position of the composition range within which the two droplet/matrix phases coexist are not affected by the change of λ according to the present results.

3.3. Influence of the additive PDMS-co-PEO

The interfacial tensions for the binary systems PEO 37/PDMS 230 and PDMS-*co*-PEO/PDMS 230 are shown in Fig. 9 in dependence on temperature together with three examples for different contents of the copolymer in the PEO-phase. σ of PEO 37/PDMS 230 decreases slightly with temperature; this is typical for systems with an upper critical solution temperature.

PDMS-*co*-PEO is a very effective additive as can be seen in Fig. 10. As little as 0.5 wt% additive reduce σ by around 60%. This concentration is already located in the region of the saturation value of σ; 0.5 wt% PDMS-*co*-PEO were, therefore, chosen for the investigation of the influence of the additive on the morphology.

The microscopic images of the blends after 1 h shearing at $5\ \mathrm{s}^{-1}$ are presented in Fig. 11 for different compositions. The presence of the additive extends the region of two coexisting droplet/matrix structures from $0.4 \leq \varphi_{\mathrm{PDMS230}} \leq 0.6$ to $0.4 \leq \varphi_{\mathrm{PDMS230}} \leq 0.7$. From the micrograph shown in Fig. 11

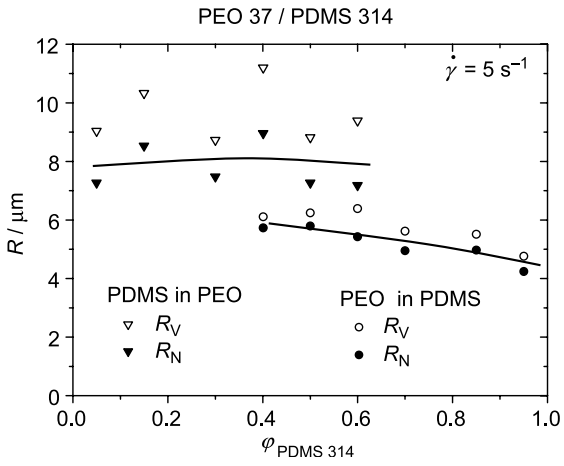

Fig. 8. Stationary drop sizes for PEO 37/PDMS 314 at $\dot{\gamma} = 5\ \mathrm{s}^{-1}$: R_V (open) and R_N (solid) in dependence of composition; triangles: PDMS drops in PEO, circles: PEO in PDMS. The line is drawn as guide for the eye.

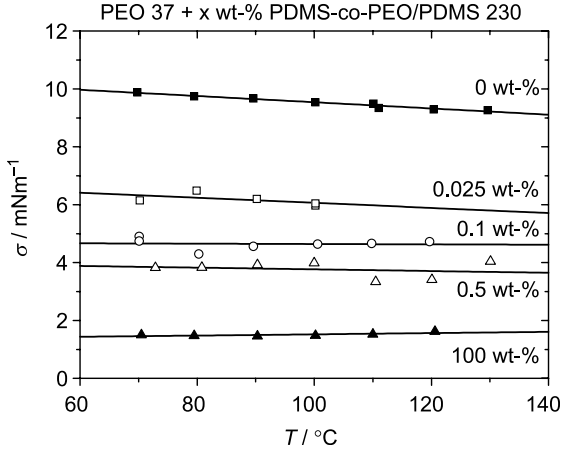

Fig. 9. Interfacial tension of PEO 37/PDMS 230 in dependence on temperature for the different indicated concentrations of PDMS-*co*-PEO. The lines are linear least square fits.

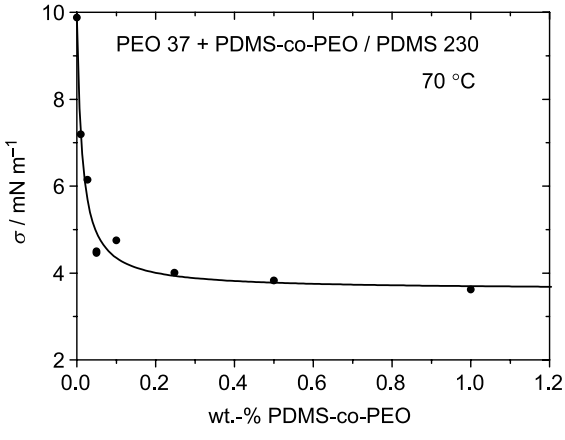

Fig. 10. σ in dependence on the addition of PDMS-*co*-PDMS to PEO. The data are fitted according to Langmuir [35,36].

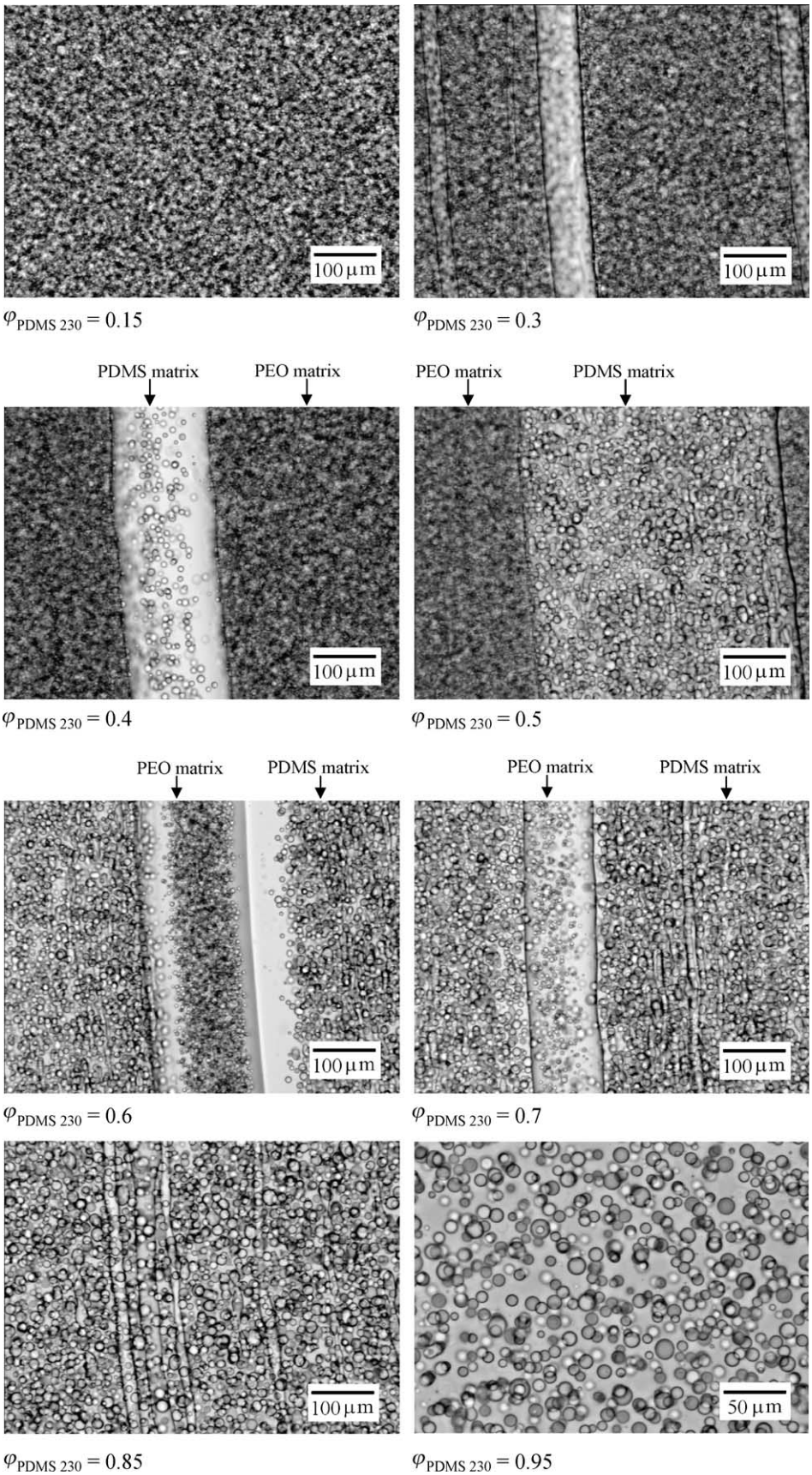

Fig. 11. Light microscopic images of different ternary mixtures (PEO 37 + 0.5 wt% PDMS-*co*-PEO)/PDMS 230 taken after 1 h shearing at $\dot{\gamma} = 5\ s^{-1}$. For taking the pictures the shear was stopped.

for $\varphi_{PDMS230}=0.7$ it can be seen that threads of the minor component not containing drops of the major component may coexist with the two droplet/matrix phases that are typical for intermediate compositions. Threads of 'pure' PDMS can also be seen at $\varphi_{PDMS230}=0.3$ and threads of 'pure' PEO at $\varphi_{PDMS230}=0.85$. These pictures could give the impression that these phases do contain drops. However, the wrong impression is obviously caused by drops that are located above or below the thread as can be ascertained by varying the focus of microscope.

The most obvious difference of the system with additive in comparison with the pure blend consists in a considerable reduction of drop size which is quantified in Fig. 12. If the copolymer-containing phase (PEO) constitutes the matrix, the drop size is approximately halved. The breakup condition (Eqs. (5) and (6)) predicts direct proportionality between σ and R, therefore, the experimentally observed reduction of σ to 40% of the original value should lead to the same decrease of R. Within the frame of the coalescence model PMI (Eq. (4)) the same diminution of σ yields a decrease of R to 58%. The observed behavior seems to be a compromise between the results of the two purebred sub-processes.

If the additive containing phase forms the drop-phase, the decrease of the drop size is not as pronounced as in the inverse case. The drop size lies just under 70% of that for the additive free system. The reason for this finding lies in the fact that the additive content within this subsystem formed by the PDMS matrix and the suspended PEO drops contains much less additive because it is almost exclusively contained in the drops.

An important difference between the blends of PEO 37/PDMS 230 with and without additive is the appearance of long and stable threads which do not contain drops of the other component, as can be seen in Fig. 11 for $\varphi_{PDMS230}=0.3$, 0.7 and 0.85. This is likely due to the reduction of σ slowing down the breakup of filaments [21,37,38]. This retardation probably also causes the observed broadening of the range of co-continuity.

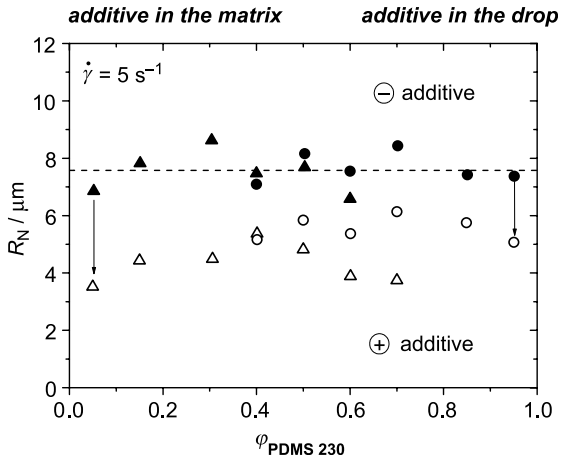

Fig. 12. Stationary drop sizes for PEO 37/PDMS 230 at $\dot{\gamma}=5\ s^{-1}$ in the absence (solid) and in the presence (open) of the compatibilizer PDMS-*co*-PEO as a function of blend composition; triangles: PDMS drops in PEO, circles: PEO in PDMS. The line is drawn as guide for the eye.

3.4. Common features

The coexisting droplet/matrix morphologies found for all blends are similar to the ones reported by Astruc and Navard [24] as intermediate structures during the shear induced phase inversion of inhomogeneous mixtures of 50% aqueous hydroxypropylcelluolose solutions (HPC50%) with PDMS at $0.55\leq\varphi_{PDMS}\leq0.67$. These authors started with a single droplet/matrix structure of HPC50%-drops in PDMS, which inverted its morphology due to the different extent of shear thinning of the two coexisting phases. This phase inversion is discussed in terms of four distinguishable steps: building of a bi-fibrillar morphology, appearance of sheets of the former matrix phase, emergence of a stripe morphology and formation of the final inverse droplet/matrix morphology. The reported stripe structures resemble the structures found for the PEO/PDMS blends in the composition range $0.4\leq\varphi_{PDMS}\leq0.6$ (the upper limit is 0.7 in the presence of PDMS-*co*-PEO). In contrast to the literature report [24], the present structures are, however, stable for long times (at least for 5 h shearing). Within one droplet/matrix phase, the processes observed for a single droplet/matrix phase (breakup and coalescence) take place unaffected by its spatial confinement in stripes. The drop sizes measured within the coexisting matrix phases do not differ from that of the single droplet/matrix structures realized for a large predominance of one component in the mixture.

The observed coexistence of two matrix phases can be regarded as a special kind of co-continuity, because it is-at least in principle-possible to extract the matrix polymers from both coexisting droplet/matrix structures. Co-continuous structures with inclusions of the counter phase are also found in extruded blends of polyamide (PA)/polystyrene (PS) blends [26], blends of polypropylene (PP)/(PS/polyphenylene-ether (PPE)) [39] and (PPE/PS)/PA blends [19]. Extraction experiments with the latter polymer mixture give only 90% co-continuity (defined as

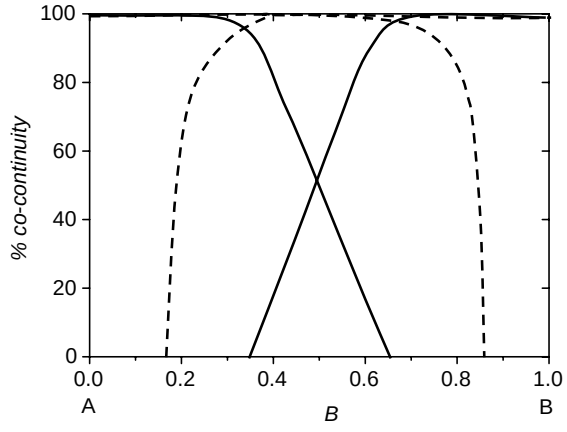

Fig. 13. Percentage of co-continuity as a function of composition. The dotted line is drawn according to Lyngaae-Jørgenssen [14] and describes the typical behavior of processed blends of incompatible polymers. The full line describes how this dependence should look like for the present morphologies. It accounts for the fact that one can never extract 100% of both components in the case of the coexistence of two droplet/matrix phases.

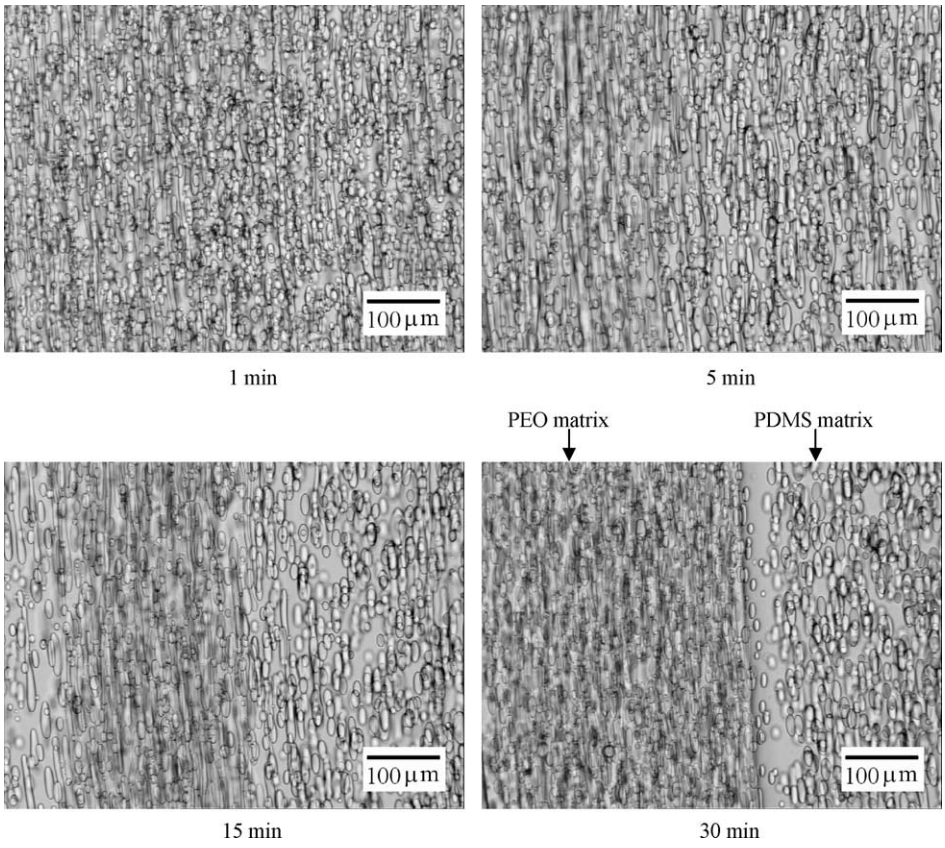

Fig. 14. Structure development for the blend PEO 37/PDMS 230 at $\varphi_{PDMS230}=0.5$ after a step down of $\dot{\gamma}$ from 15 to 5 s^{-1}.

the amount of a certain phase which can be extracted by a specific solvent, divided by the total amount of this phase originally present in the blend) in the phase inversion region; this finding indicates that a part of this phase is inaccessible to the solvent.

In Fig. 13 we present a qualitative comparison of the composition dependence of the degrees of co-continuity typically for typical industrial polymer blends (drawn according to Lyngaae-Jørgensen [14]) and with the dependence expected for the present systems.

There exist at least two different possible paths for the formation of co-continuous structures. One consists in the building of sheets of the matrix phase [23–26] and the other option lies in the coalescence processes of more or less elongated drops [19,21,22]. The latter mechanism is proposed in literature especially for blends with high interfacial tension, like the present one, because large σ values reduce the stability of long extended structures [19,21,22].

Tol et al. [19] consider co-continuity in a blend with high σ as the result of the recombination and coalescence of the collapsed threads. Li et al. [21] investigated blends with large differences in σ and state that in blends with high σ the lifetime of the threads is lower than for blends with low σ. For large interfacial tension fiber formation and the establishment of continuity will proceed via droplet–droplet interactions instead of the coalescence of long threads. The latter mechanism is proposed by Luciani and Jarrin [22].

Some examples for the development of stripe morphologies are shown in Fig. 14 for $\varphi_{PDMS230}=0.5$ and Fig. 4 for $\varphi_{PDMS230}=0.4$. These pictures suggest that the stripes are formed via coalescence. In our case the small threads, existing at the beginning of the experiments, are not stable but transform into stripes of inverse droplet/matrix structures, which are stable against breakup due to their large lateral dimensions.

With all systems under investigation the droplet density of component A in a matrix of B (coexisting with a second droplet/matrix phase B in A) increases with the augmentation of φ_B until the B in A phase disappears and we are back to a single droplet/matrix structure. The following kinetic considerations may tentatively explain the composition limits for the coexistence of two droplet/matrix phases. The present experiments start with a single droplet/matrix phase that contains the entire minor component as small drops, which were created during the sample preparation by stirring with a spatula. For sufficiently low volume fractions of the minor component this morphology is retained as the system is sheared. However, beyond a characteristic degree of filling of the matrix with these droplets, coalescence processes will become so dominant that part of these droplets form larger stripes, which are stable against the Rayleigh instability. These stripes constitute a second matrix containing some drops of the former matrix phase. The drop densities near

the boundaries between the matrix phases may decrease with time due to their migration into the neighboring continuous phase.

Acknowledgements

The authors would like to thank the 'Arbeitsgemeinschaft industrieller Forschungsvereinigungen', which finances this research (project number 13792N).

References

[1] Taylor GI. Proc R Soc London A 1934;146:501–23.
[2] Rumscheidt FD, Mason SG. J Colloid Sci 1961;16:238–61.
[3] Grace HP. Chem Eng Commun 1982;14:225–77.
[4] DeBruijn RA. Thesis Eindhoven University of Technology; 1989.
[5] Chesters AK. Trans I Chem E A 1991;69:259–70.
[6] Elmendorp JJ, Van der Vegt AK. Polym Eng Sci 1986;26(19):1332–8.
[7] Janssen JMH. Thesis University of Technology, Eindhoven; 1993.
[8] Minale M, Moldenaers P, Mewis J. Macromolecules 1997;30(18): 5470–5.
[9] Vinckier I, Moldenaers P, Terracciano AM, Grizzuti N. AIChE J 1998; 44(4):951–8.
[10] Lyu SP, Bates FS, Macosko CW. AIChE J 2002;48(1):7–14.
[11] Tucker CL, Moldenaers P. Annu Rev Fluid Mech 2002;34:177–210.
[12] Ziegler VE, Wolf BA. Polymer 2005;46:9265–73.
[13] Ziegler VE, Wolf BA. Macromolecules 2005;38:5826–33.
[14] Lyngaae-Jørgensen J, Utracki LA. Makromol Chem, Macromol Symp 1991;48/49:189–209.
[15] Bourry D, Favis BD. J Polym Sci, Part B: Polym Phys 1998;36(11): 1889–99.
[16] Chuai CZ, Almdal K, Lyngaae-Jørgensen J. Polymer 2003;44(2): 481–93.
[17] Favis BD, Chalifoux JP. Polymer 1988;29:1761–7.
[18] Andradi LN, Hellmann GP. Polym Eng Sci 1995;35(8):693–702.
[19] Tol RT, Groeninckx G, Vinckier I, Moldenaers P, Mewis J. Polymer 2004;45(8):2587–601.
[20] Potschke P, Paul DR. J Macromol Sci-Polym Rev 2003;C43(1):87–141.
[21] Li JM, Ma PL, Favis BD. Macromolecules 2002;35(6):2005–16.
[22] Luciani A, Jarrin J. Polym Eng Sci 1996;36(12):1619–26.
[23] Lazo NDB, Scott CE. Polymer 2001;42(9):4219–31.
[24] Astruc M, Navard P. J Rheol 2000;44(4):693–712.
[25] Lazo NDB, Scott CE. Polymer 1999;40(20):5469–78.
[26] Sundararaj U, Macosko CW, Shih CK. Polym Eng Sci 1996;36(13): 1769–81.
[27] Wu S. Polymer interface and adhesion. New York: Marcel Dekker; 1982.
[28] Song B. Thesis TU Berlin, Berlin; 1994.
[29] Jorzik U, Wolf BA. Macromolecules 1997;30(16):4713–8.
[30] Chesters AK. In: International conference turbulent two phase flow systems, Toulouse, France; 1988, 1988. p. 234.
[31] Janssen JMH, Meijer HEH. Polym Eng Sci 1995;35:1766–78.
[32] Grizzuti N, Bifulco O. Rheol Acta 1997;36(4):406–15.
[33] Minale M, Mewis J, Moldenaers P. AIChE J 1998;44(4):943–50.
[34] Rusu D, Peuvrel-Disdier E. J Rheol 1999;43(6):1391–409.
[35] Langmuir IJ. J Am Chem Soc 1916;38:2221.
[36] Langmuir IJ. J Am Chem Soc 1918;40:1361.
[37] Tomotika S. Proc R Soc London. A 1936;A153:302–18.
[38] Tomotika S. Proc R Soc London, Ser A: Math Phys Sci 1935;A150: 322–37.
[39] Everaert V, Aerts L, Groeninckx G. Polymer 1999;40(24):6627–44.